

SOLAR POWERED MULTIPURPOSE REMOTELY POWERED AIRCRAFT

Worcester Polytechnic Institute
Mechanical Engineering Department
Worcester, Massachusetts

Dr. A. N. Alexandrou, Dr. W. W. Durgin, Dr. R. F. Cohn, Dr. D. J. Olinger
Charlotte K. Cody, Teaching Assistant
Agnes Chan, Kwok-Hung Cheung, Kristin Conley, Paul M. Crivelli, Christian T. Javorski,
Nancy P. Torrey, Michael L. Traver

Abstract

Increase in energy demands coupled with rapid depletion of natural energy resources have deemed solar energy as an attractive alternative source of power. The focus of this work was to design and construct a solar powered, remotely piloted vehicle to demonstrate the feasibility of solar energy as an effective, alternate source of power. The final design included minimizing the power requirements and maximizing the strength-to-weight and lift-to-drag ratios. Given the design constraints, *Surya* (the code-name given to the aircraft), is a lightweight aircraft primarily built using composite materials and capable of achieving level flight powered entirely by solar energy.

Introduction

Mission Requirements

As civilization enters the 21st century, considerations for alternative energy sources are becoming necessary. Natural energy sources such as coal, oil, and fossil fuels are quickly depleting. In addition, they are harmful to the environment. Their use has caused a substantial increase in air pollution, and they have thus been major contributors to the greenhouse effect. Although nuclear energy is immediately available, high operational risks and environmental issues have made it a questionable option. Solar energy is not only pollution-free, but it is also available in abundance. Proper utilization of the sun's energy can result in an inexpensive and effective power source. One of the main objectives of this project was to demonstrate the effectiveness and feasibility of using solar energy to power an airborne vehicle. The final

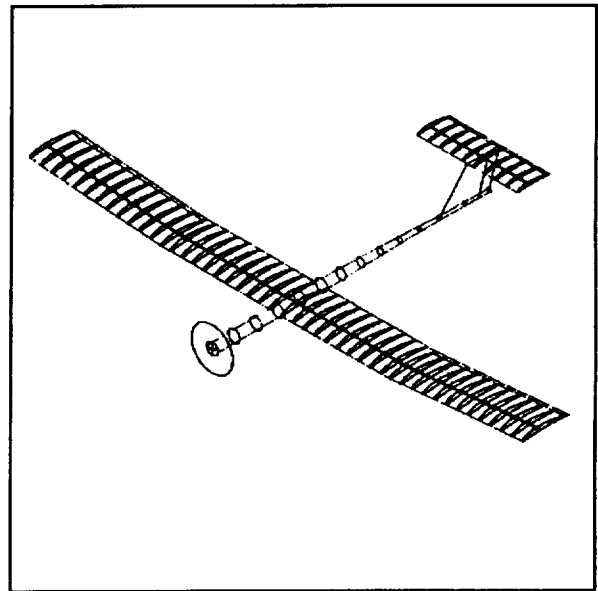


Fig. 1 *Surya* Isometric View

Table 1 General Data

Weight	W_{gross}	40 N
Wing Area	S	1.48 m ²
Wing Loading	W	27.03 N/m ²
Aspect Ratio	AR	8.25
Wingspan	b	3.5 m
Cruise Altitude	h	50 m
Cruise Velocity	V	7 m/s
Design Lift Coeff	C_L	0.83
Design Lift-to-Drag	L/D	15.75
Cruise Power Req'd	P	15.9 W
Design Load Factor	n	7

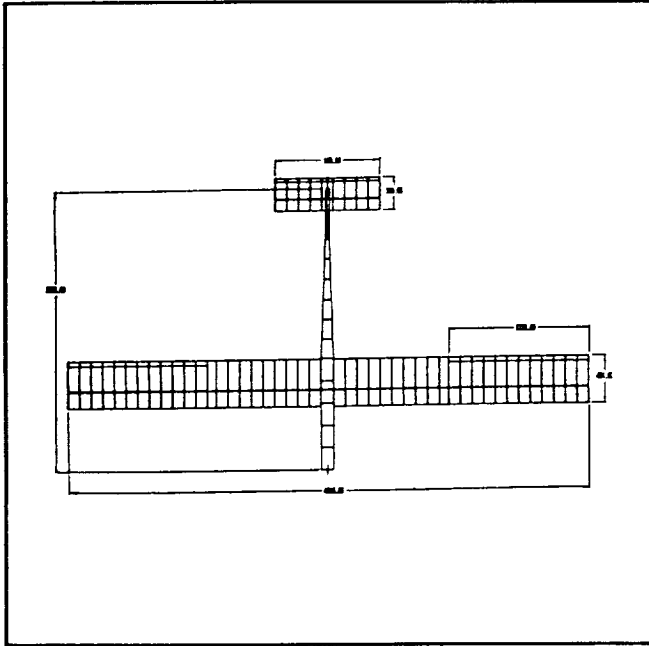


Fig. 2 *Surya* Top View

configuration of the solar plane was optimized for minimum level flight power.

Aircraft Configuration

The proposed vehicle is shown in Figures 1 and 2. General data and design parameters are summarized in Table 1.

The wing has a span of 4.5 m, a chord length of 42.4 cm, an aspect ratio of 10.61, and is positioned at a geometric attack angle of 4 degrees. A lift coefficient of 0.8274 is generated by the wing during level flight. The tail is oriented at an angle of attack of 0 degrees and its lift coefficient is 0.4053. The tail efficiency is assumed to be 0.85.¹ The overall configuration has a total lift coefficient of 0.8816, a total drag coefficient of 0.0451, yielding a L/D ratio of 19.548.

The wing design includes a dihedral of 2.5 degrees. The vertical stabilizer has an effective area of 900 cm², the rear half being the rudder. Situated 1.6 meters behind the aerodynamic center of the wing, the horizontal stabilizer spans one meter and is composed of a NACA 6409 airfoil with a 30 cm chord. The rear quarter of this chord is a hinged flap which serves as the elevator. The ailerons are

located on the modular wing sections, occupying the aft 12% of the chord and spanning the entire length. To ensure pitch stability and optimum lift for the plane as a whole, the center of gravity is maintained a tenth of the wing's chord behind its aerodynamic center. The location of the electronics harness in the nose of the fuselage is adjustable and can be moved either forward or backward to insure the center of gravity is positioned to maintain static stability.

A total of 120 solar cells are contained within the wing of *Surya*. This number was determined through required power estimations. Conservative estimates predicted about 100 watts for the array output at any given time during flight. Although this number is rather high, the actual amount of power delivered to the motor and propeller was much less. On an open circuit, the cells developed a potential of 5.8 volts while producing approximately 19 amps of current when short circuited. As load is applied to the array, these values drop to 4.7 volts and between 12 and 14 amps. To produce the required power, 12 arrays containing 10 cells were constructed. The five volt potential is the result of the 10 cells wired in series with each individual cell producing 0.5 volts. The 12 amp current is generated by wiring the 12 sub-arrays in parallel at 1 amp each.

The solar array is split into three rows per wing section. The leading edge row is placed underneath the skin to preserve the integrity of the front part of the airfoil, where it is most crucial. The trailing rows adhere directly to the skin on the outside of the wing to increase power production. The first row sits at an angle of 12° with respect to the chord, while the back rows sit at an angle of 6°. As a result, optimum power is produced by the array during level flight with the plane flying directly away from the sun.

Surya's total coefficient of lift was estimated at 0.88, and both the tail and the wing act as lifting surfaces. With a weight of 52 N and an estimated parasitic drag coefficient at 0.148, the plane is expected to have a minimum flight speed of 7.1 m/s and a minimum required power to achieve this speed of 18.8 Watts.

The climb capability of the plane is strictly determined by the amount of excess power available. *Surya's* climb rates vary depending on the output of power from the

solar cells at that time interval, and the position of the plane relative to the sun.

Banking and turning are basic maneuvers at which the plane must remain in level flight. Since the flight velocity of the solar plane is low, the banking angles are small. With small banking angles between 3 and 4 degrees, the turn radii necessary are 89 and 67 m respectively. Hence, the proposed spiral climb scheme for the 50 m altitude climb can be accomplished in about five minutes within a 200 m length field.

Table 2 Wing Component Masses

Wing	Mass (g)	% Wing
Carbon Composite Spars	478.0	15.9
Ribs	132.0	4.4
Leading Edge	116.0	3.8
Trailing Edge	58.0	1.9
Ailerons	99.0	3.3
Spar Webs	44.8	1.5
Skin (Mylar)	254.4	8.4
Wing Tips	36.1	1.2
Solar Cells	1142.0	37.9
Servos	43.0	1.4
Wiring	148.0	4.9
Reinforced Rib	158.0	5.3
Modular Tube Connection	107.0	3.6
Landing Gear	58.0	1.9
Miscellaneous	139.0	4.6
Total	3013.4	100

Design and Analysis

Aircraft Sizing and Weight Estimation

Preliminary component sizing was dictated by set parameters such as the chosen airfoil, the size of the solar cells, and the desired lift-to-drag ratio. The optimization of the design included the minimization of the power requirements and the maximization of the strength-to-weight and lift-to-drag ratios. The resulting configuration has a wing span of 4.5 m, a tail span of 1 m, and a fuselage

length of 2.5 m. Due to the large span, the wing was constructed in modular sections for storage purposes. Tables 2 through 4 break down the masses of individual elements of the plane showing their percent contribution to each section of the aircraft.

Table 3 Fuselage Component Masses

Fuselage	Mass (g)	% Fuse
Carbon Composite Frame	900.0	48.9
Servo	21.5	1.2
Wiring	98.3	5.3
Motor	245.7	13.3
Nose Cone	56.8	3.1
Propeller	42.9	2.3
Receiver Battery	101.1	5.5
Receiver	44.0	2.4
On/Off Switch	63.3	3.4
Emergency Batteries	238.0	12.9
Miscellaneous	32.0	1.7
Total	1843.5	100

Aerodynamic Design and Analysis

The wing has a rectangular platform with a wing span of 4.5 m and a chord length of 0.424 m. The aspect ratio of the wing is 10.61 and the geometrical angle of attack is 4° . The wing generates a lift coefficient, C_L , of 0.8274 at level flight conditions. The tail has a rectangular platform, a tail span of 1 m, and a chord length of 0.3 m. The resulting aspect ratio of the tail is 3.333. At level flight conditions, the geometrical angle of attack of the tail is 0° and the C_L is 0.4053. The tail efficiency was assumed to be 0.85.¹ With this configuration, the aircraft has a total lift coefficient of 0.8816 and a total drag coefficient of 0.0451. As a result, the total lift to drag ratio is equal to 19.548.

The chord Reynolds number is relatively low since a solar aircraft has a fairly slow cruise velocity. Theoretically, viscous effects dominate the flow at low Reynolds numbers, thus resulting in flow separation and a laminar separation bubble. However, at Reynolds number of 200,000 or higher, a turbulent boundary layer develops and gives more resistance to flow separation

during the pressure recovery. For this reason, it was decided to operate the plane at a Reynolds number based on the chord of about 200,000. In addition, the effects of compressibility are neglected in the entire aerodynamic analysis, since the Mach number during level flight is much less than 0.3.

The NACA 6409 was chosen as the airfoil section for the wing and the tail. It has a 9% maximum thickness and a 6% maximum chamber at a distance of 40% of the chord from the leading edge. Figure 3 shows the experimental lift and drag characteristic of the NACA 6409 airfoil at the Reynolds number of 200,100.² The sectional lift curve slope of the airfoil is about 5.17 per radian between an angle of attack of -0.87 and 7.32 degrees. At an angle of attack of 9.32 degrees, the sectional lift coefficient reaches a maximum value of 1.342. Meanwhile, the sectional drag coefficient varies parabolically and has a minimum drag coefficient of 0.0112 at an angle of attack of 1.20 degrees. The lift to drag ratio of the airfoil is calculated and summarized in Figure 4. As shown in the figure, the airfoil provides a constant high lift to drag ratio between the angles of attack of 2 and 8 degrees and therefore allows for a wide range of favorable operating conditions.

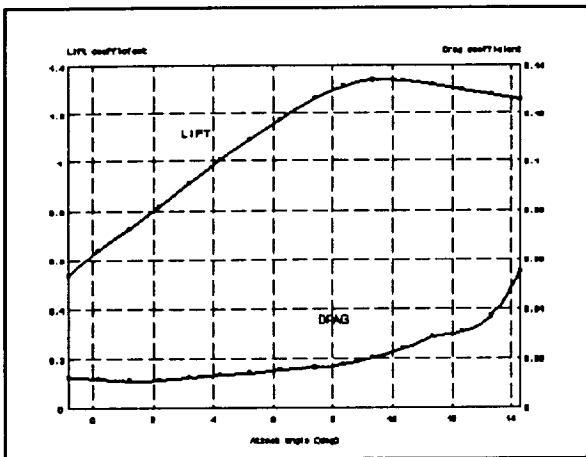


Fig. 3 Sectional Lift and Drag Coefficients

In order to increase the power generated by the solar propulsion system, cells are placed on the surface of the wing. Since the solar cells are flat and not flexible, the shape of the airfoil is slightly changed. As a result, the sectional characteristics of the airfoil are affected. By

using the vortex panel method,³ the inviscid pressure distribution of the original NACA 6409 was calculated as shown in Figure 5. In the figure, it is clearly shown that the majority of the lift is generated in the front 40% of the airfoil. Therefore, in order to minimize the aerodynamic effects due to the solar cells placement, the cells were placed behind a distance of 40% of the chord from the leading edge (see Figure 6). The inviscid pressure distribution of the airfoil which has the solar cells on the back is shown in Figure 7. At an angle of attack of 4o, the difference between the inviscid lift coefficients of the original airfoil and the one which has solar cells on the back is only about 0.25%.

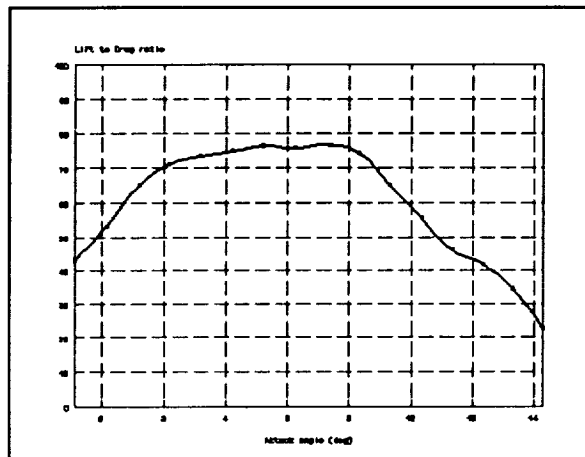


Fig. 4 Sectional Lift-to-Drag Ratio

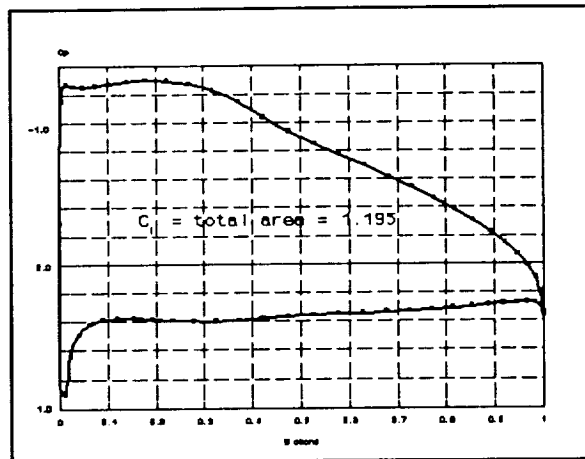


Fig. 5 Inviscid Pressure Distribution

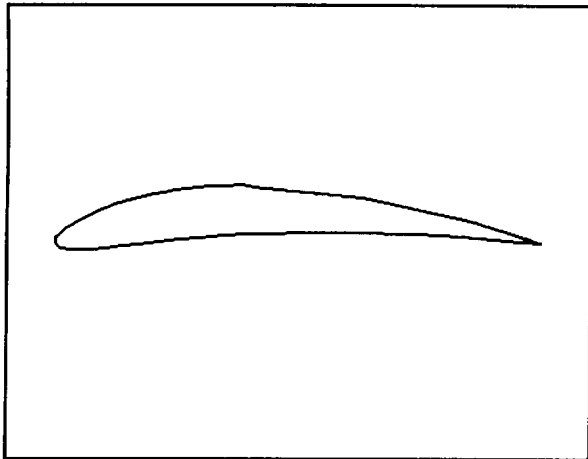


Fig. 6 Modified NACA 6409 with Flattened Back

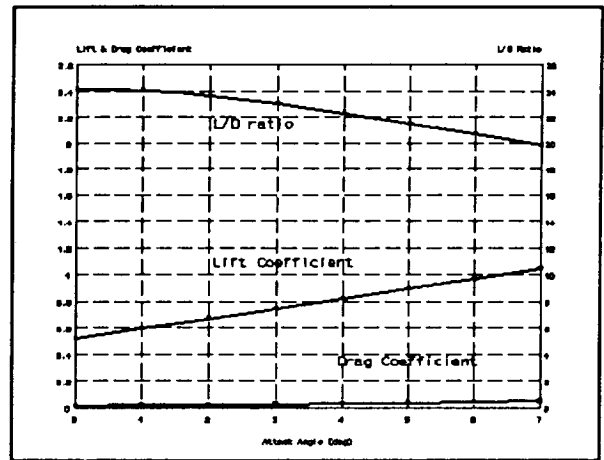


Fig. 8 Lift and Drag Characteristics of the Finite Wing

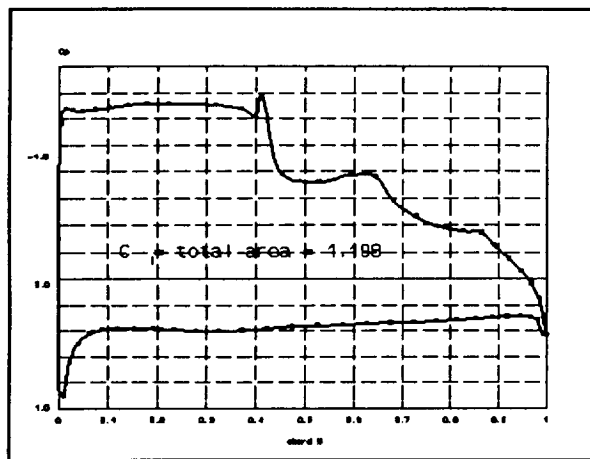


Fig. 7 Inviscid Pressure Distribution for Modified NACA 6409

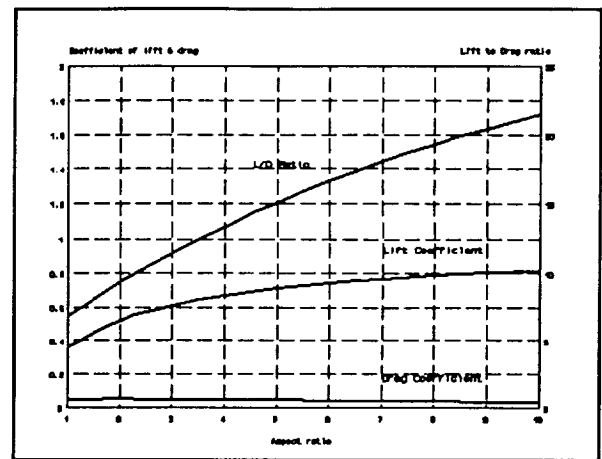


Fig. 9 Effects of the Aspect Ratio on Lift and Drag

Assuming the flow does not separate before the first 40% of the chord, the aerodynamic characteristics of the modified airfoil are apparently similar to the original NACA 6409. Therefore, the experimental data of the NACA 6409 airfoil are assumed to be valid for the design.

Using the Glauert Method and the modified flat plate theory,¹ the finite lift and drag coefficients of the wing and tail are determined. Figure 8 shows the finite lift and drag characteristic of the wing at different attack angles. In addition, the aspect ratio effects or the L/D ratio are

investigated. With a higher aspect ratio, the wing behaves closer to the predicted performance of the airfoil section. As a result, the wing generates more lift and experiences less induced drag. Figure 9 shows clearly that the lift to drag ratio increases while the aspect ratio of the wing increases.

The power required for level flight at different velocities is summarized in Figure 10. As the figure shows, the optimum level flight speed is 6.388 m/s and the corresponding attack angle is 6.77 degrees. At this

condition, the power required for level flight is equal to 18.682 Watts. Due to safety considerations, it was decided to operate at an attack angle of 4° , with the corresponding cruising speed is 7.104 m/s. The required power is 18.839 Watts, which is 0.84% higher than the power required at the optimum condition.

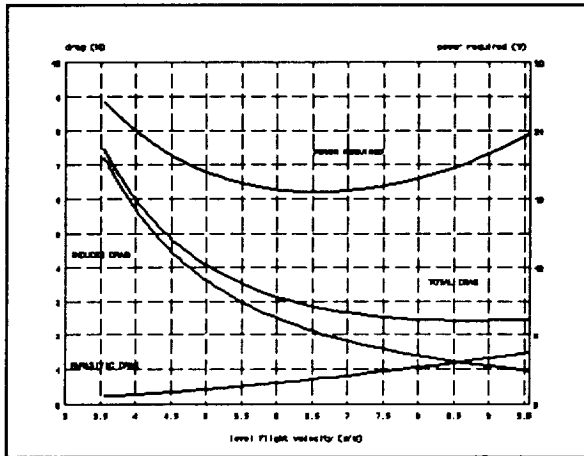


Fig. 10 Power Required vs Flight Velocity

Structural Design and Analysis

The main supporting structure of the wing is a rigid tube running the length of the span, effectively acting as a wing spar. The outer diameter of the tube was limited by the thickness of the airfoil. The thickness of the tube was determined by a simplified stress analysis of the loads applied to the spar.

A simplified half wing loading model was developed to estimate the maximum stress on the wing spar (see Figure 11). The carbon spar was to assume all of the loads due to the lift generated. The wing was modeled as a cantilevered beam with a distributed load, and a moment load applied at the free end. The lift of 48.3 Newtons was represented by a distributed load of 10.73 N/m acting along the full span. This load produces an effective moment of 5.36 N-m located at the connection point, shown at the free end of the beam. These calculations were adjusted to account for the potential gust load the wing may endure. With a gust load factor of 3, the loads were increased to a distributed load of 32.19 N/m and an effective moment of 16.09 N-m.

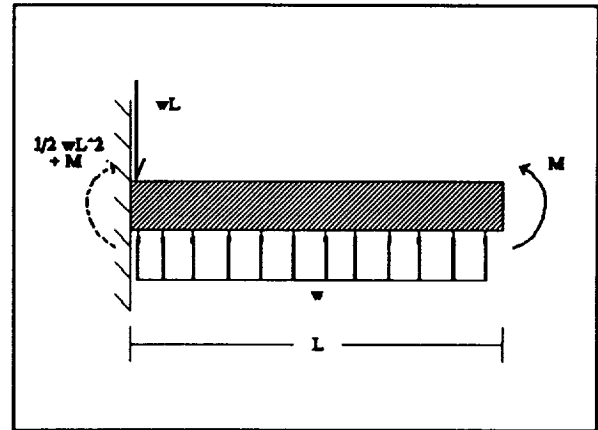


Fig. 11 Wing Loading Model

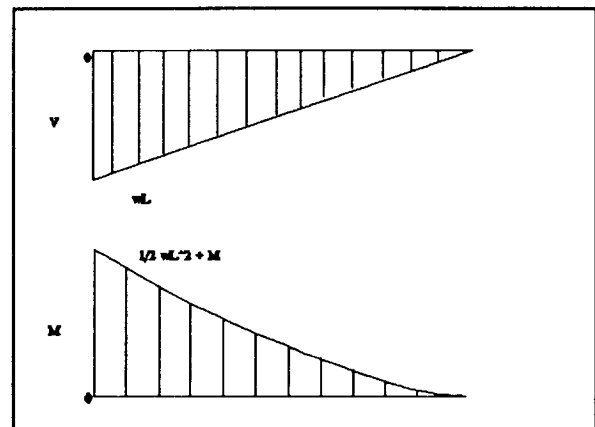


Fig. 12 Shear and Moment Diagrams

The shear and moment distributions of the wing are illustrated in Figure 12. The locations of maximum shear and maximum bending moment were determined from these diagrams, 40.24 N and 41.24 N-m respectively. The maximum normal stress resulting from expected loads and the material properties of carbon fiber were considered; shear stress was determined to be negligible in comparison. Carbon composite spars were constructed and tested to obtain accurate material properties. Considering the maximum expected load and a safety factor of 1.2, the maximum allowable stress for the spar

was calculated and determined to be $2.75E+8 \text{ N/m}^2$. The minimum required spar thickness was iteratively determined. A wing spar having an outer diameter of 20.1 mm, 0.53 mm thickness (3 layers of fabric), and capable of withstanding a maximum load of $3.303E+8 \text{ N/m}^2$ was constructed. The tail was modeled and analyzed similarly to that of the wing, differing only by the absence of a moment at the free end. The lift on the tail was calculated to be 3.7 Newtons and a distributed load of 3.7 N/m was modeled. The resulting tail spar dimensions are an outer diameter of 1.38 cm and a thickness of 0.53 mm. The sizing of the fuselage was dependent on the placement of the tail and the area required to house the electronics and was determined to be 2.5 meters. The anterior portion of the fuselage is 10.5 cm in diameter, which was determined by an estimation of the size of the electronic components. This diameter gradually decreased with length in order to minimize weight. The posterior segment has a diameter of 3 cm. This value was determined to be the minimum within the margin of safety. The required thickness of the fuselage wall for this design was 0.36 mm (2 fabric layers).

Material Selection

The material selection process played a key role in the design. Since the limited power available from the solar cells mandated weight minimization, effective material selection was crucial in the design process. While the weight of the structure needed to be minimized, a high strength material was desired to withstand the applied loads. This dictated the use of composite materials because they exhibit a high strength to weight ratio.

Many composite fabrics were tested including carbon, kevlar, and fiberglass. Carbon was selected due to its high strength-to-weight ratio and inherent rigidity. Consequently, the wing spar, tail spar, and fuselage were constructed using this material. Furthermore, a number of different spar configurations were tested to determine the material constraints at different loads. These tests led to the selection of a hollow circular cross-section. Sample hollow rod configurations were tested to determine the thickness of the tube required to withstand the expected stress.

The vertical stabilizer which supports the tail spar was constructed using a foam structure that was reinforced with carbon composite fabric on both sides. The carbon

composite provided the strength needed to support the tail, and foam was used as a spacer.

Since the wing spar was modular, a connecting support was used to form the dihedral angle in the wing and withstand the load applied at the connection. The modular connection supports utilized a foam and carbon composite combination much like that of the vertical stabilizer with foam sandwiched between two layers of carbon composite fabric. Foam was used as a spacer in the vertical stabilizer and modular connection supports because of its low density, making it the most lightweight material used in the plane. The carbon composite fiber and foam combination proved to be ideal when used on components that were designed to withstand pure bending loads. Foam was used to construct components without structural applied loads, such as the solar cell braces, nose cone, and wing tips.

Balsa wood was utilized for many components that sustained small loads and required a precise shape. Since balsa is the lightest of all wood and very easily shaped it was favored over foam. Balsa wood was used for components such as the ribs, the leading and trailing edges, the ailerons, the elevator, and the horizontal stabilizer. The ailerons and the horizontal stabilizer utilized balsa wood in a truss structure designed as an extension of the airfoil.

Heat shrinking mylar was used for vehicle's skin. It was necessary to use a material with a high transmissivity on the top of the wing allowing the sunlight to reach the solar cells underneath the skin, but at the same time the material had to be strong enough to sustain the shape of the airfoil it formed. Another concern about the material of the skin was a desired resistance to tear as deformation of the wing was experienced. Mylar becomes rigid after being heat shrunk over a surface but it remains adequately flexible enough to deform.

Propulsion System Design and Integration

The modified remote control radio system and the necessary hardware for controlling deflecting surfaces and switches via servo-motor, shown in Figure 13, is the essence of the controls and interface scheme.

The Astro Cobalt 05 electric, geared motor and a two-bladed, folding propeller with a diameter of 33 cm and

pitch of 16.5 cm manufactured by Aero-Haute were chosen for their combined efficiency. A combined contour plot of electrical input power, shaft torque, shaft RPM, and motor efficiency versus voltage and current is shown in Figure 14. Several motor-propeller combinations were tested in the WPI wind tunnel under conditions similar to those in flight. Figure 15 illustrates the results of the tests performed for the chosen motor-propeller combination.

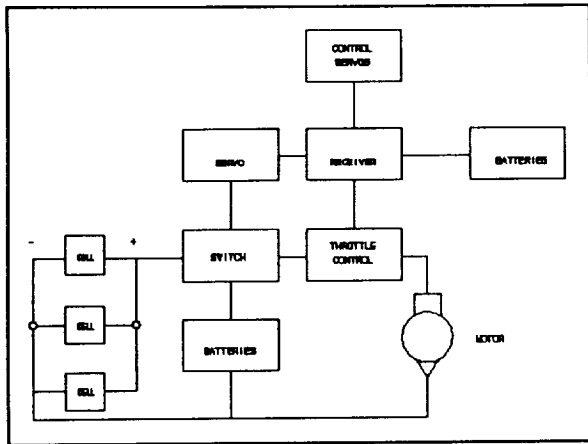


Fig. 13 Controls Layout

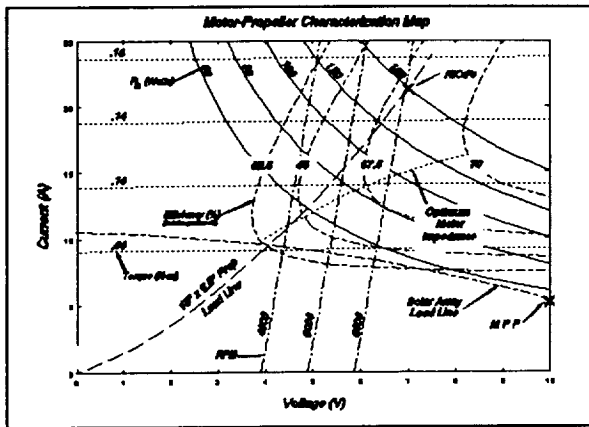


Fig. 14 Combined Contour Plot for Design Motor-Propeller

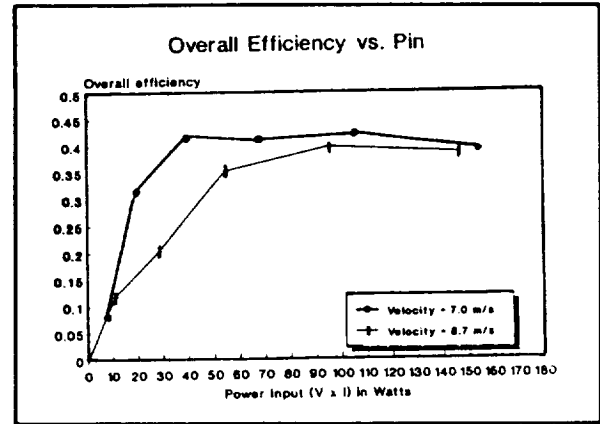


Fig. 15 Efficiency vs Power Input for Design Motor-Propeller

As a safety feature, there is a NiCad battery pack installed in the fuselage of the plane. At full power the batteries produce eight to nine volts and upwards of 20 amps. The use of these batteries is limited as their lifespan is not more than five or six minutes. A manual switch shifts the power source from the cells to the batteries. The batteries can be slowly recharged up to five volts during glides if the motor is turned off. A diode connected between the cells and the batteries prevents the batteries from charging the array.

The control surfaces are operated by remote control through the use of the servos. A very small current needed to run each servo is controlled by its own channel frequency. Both ailerons are wired into the same channel to act in opposite directions. The rudder and the horizontal stabilizer are wired separately and receive their own channels. All servos are wired to the receiver box where they pick up the signals for operation. The receiver itself needs a small battery pack to operate. These are four rechargeable 1.2 volt cells. There are enough channels available on the receiver not only to handle the control surfaces, but also the throttle and the main power switch.

The power requirements for level flight are met through the utilization of silicon solar cells. The level flight speed of 7.1 m/s and the weight of 52 Newtons dictate a

minimum power requirement of 18.8 Watts. The solar array implemented on the plane produces approximately 108 Watts for the test flight date (April 11, 1992). This power production is calculated with the plane flying away from the sun thus exposing the greatest cell area to the sun's rays. The power produced for the plane flying toward the sun is approximately 98 Watts. These values do not include the power losses suffered in the motor/propeller transmission, since even an optimized power train reduces the power by more than half.

A number of parameters control the amount of power produced as well as the construction of the array. The weight of the cells is considerable and compose a large portion of the overall weight of the plane. Therefore, the cells must produce more power to the overall thrust than they contribute to weight. The photovoltaic cells are rated at an efficiency of 12.5%, determined at ideal conditions in a laboratory. The actual efficiency is lower due to design conditions. Substantial power loss occurs due to impedance matching and resistance of the wiring. The wing geometry allows only a limited number of possible array configurations and limits the number of possible voltage-current options.

A basic solar cell (Figure 16) consists of two layers of Silicon glass. The top layer is doped with Phosphorous to produce an excess of electrons while the bottom layer is doped with Aluminum to produce an abundance of electron holes. As photons strike the surface of the cell, they knock loose the excess electrons in the SiP bond. The net effect is the creation of free conduction electrons and positively charged holes which generate an electric potential between the top and bottom layers. Basic inefficiencies in this process are reflection and recombination of the photons striking the cell. Also, some photons do not possess the energy to knock loose the electrons thus rendering some of the incident light ineffective. Other photons possess too much energy and waste the excess when striking the electrons.⁴

The amount of solar power reaching the cells on a given day relies on many geometric and atmospheric variables. Obviously, a clear sunny day is better than an overcast day, yet summer months are not necessarily better than winter. Air pollution and building reflection contribute to the decrease in power availability. However, the position of the sun relative to the cells is the dominating factor.

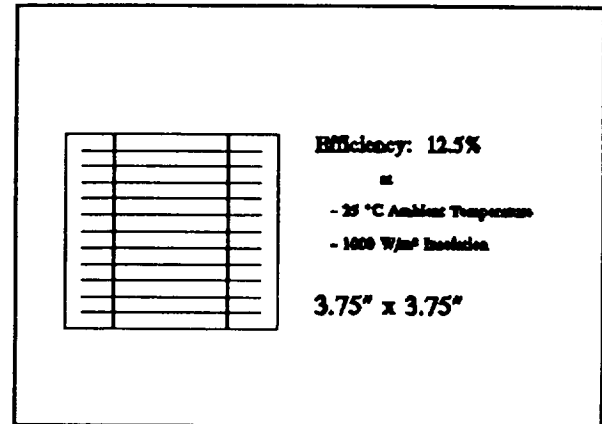


Fig. 16 Mobil Solar Silicon Photovoltaic Cell

The power received is not the available energy, since the cells can only convert around 12.5% to electric power. This electric power is eventually transformed into thrust through the motor and propeller configuration. Therefore, the cells must produce enough power to overcome the losses induced by the power train to sustain level flight. Assuming that the power train will convert only about 20 to 30%, this target and the estimated power produced dictate the initial number of cells to be installed upon the plane. With 18.8 Watts needed to fly the plane and the wing geometry in mind, the number of cells to be placed upon the wings is 120.

A random sampling of solar cells was taken to the roof of Salisbury Laboratories on the 18th of November 1991, and tested for their open circuit voltage and short circuit current. On that day, the individual cells produced approximately 0.5 Volts and, depending upon the orientation, 0.6 - 1.1 Amps. A similar test was performed on February 6, 1992. This test used a ten cell array; the characteristic I-V curve and maximum power point for the array were determined (see Figures 17 and 18). The clear mylar skin array reduces the amount of current produced, thus affecting the power available. For this reason, as many cells as possible were placed on the outside of the wing to maximize power production. Each array on the plane must have an equal number of cells, avoiding losses due to internal circuits.

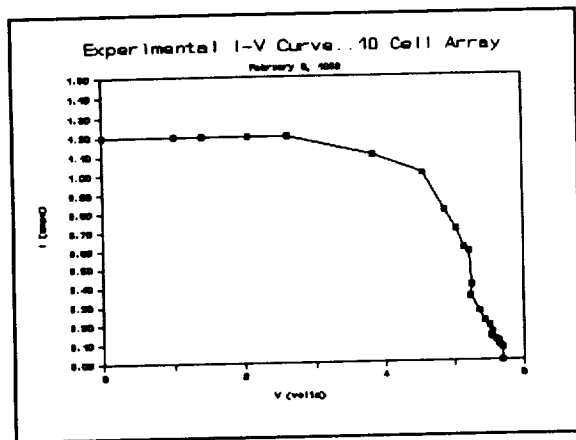


Fig. 17 Experimentally Determined I-V Curve

The array was configured to accommodate the desired wing geometry and the predicted load. The chord of the wing allows for the placement of three rows of cells along the entire span. In order to maintain the desired aerodynamic characteristics of the aircraft the first row on the leading edge is placed underneath the wing skin. The second and third rows are placed on the outside of the wing on the rear of the airfoil. The arrays should be angled to receive the greatest amount of sunlight at any given time. On a stationary platform the array would be angled at about 45° to the horizontal. Since the plane is constantly moving in the horizontal and vertical planes, the best inclination is to place the array close to the horizontal. The front cells are inside facing forward and placed as close to horizontal as the wing geometry will allow at an angle of 12° to the chordline. The rear cells are subject to geometric constraints as well and are placed directly onto the flatback airfoil at angles of approximately 6° to the chordline.

The constructed array consists of twelve sub-arrays of ten cells placed on both the main and modular sections of the wing and integrated into the propulsion system. All twelve are connected in parallel to generate an anticipated 5 Volts and 12 Amps.

Construction Process

The wing and tail supporting spars and the tapered fuselage were uniquely constructed using a woven carbon

fabric and West System epoxy to create durable, lightweight components. A piece of ordinary PVC wrapped in mylar, to prevent any adhesion to the resultant carbon tube, served as a mold for the spars. The fuselage mold was constructed using PVC tubing of the desired diameters with a tapered section made of foam connecting them. Wrapping the carbon fabric about the molds and applying epoxy generated components with desirable strength-to-weight characteristics. A microlyte filler was applied to the finished carbon structure to smooth out the imperfections and reduce the drag on this member. The main wing was connected to the fuselage by drilling a hole through the fuselage and passing the wing tube through the center of the body. The connection was reinforced using carbon fiber sleeves. Subsequent tasks included gluing the ribs to the wing spar, applying the mylar, and wiring all of the electrical components and solar cells.

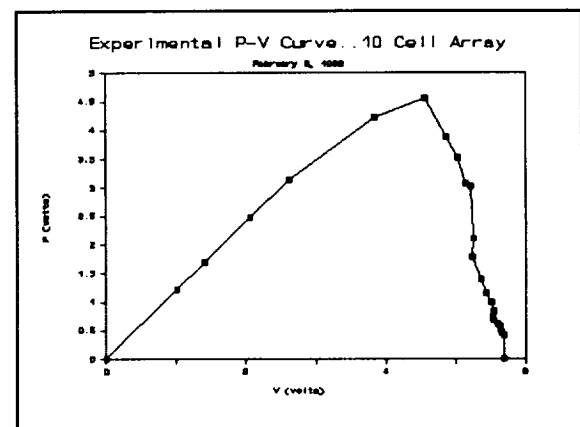


Fig. 18 Experimentally Determined P-V Curve

The solar cell array was connected entirely by hand. Each of the 120 cells donated by Mobil Solar arrived naked. Two metal ribbon leads were soldered to one side of every cell. This was accomplished with a small soldering iron and 60/40 lead/tin solder. Once completed, ten unit arrays were assembled by soldering the leads of one cell to the back of another in a long chain. Integrating the cells of the wing created a slight problem. The front row could be easily placed upon small styrofoam shelves underneath the coating of plastic, but the back rows needed some way to adhere directly to

the covering. Fortunately, a roll of double-sided adhesive was donated by Flexcon Corporation. This adhesive was applied in two half-inch strips to the backside upon which the array rested. To prevent disintegration of this bond and the cells, a small strip of plastic ran along the leading edge of the array and joined the wing approximately 1.5 inches in front of the cells. This prevented the airstream from finding its way underneath the cells and ripping them off.

Stability

Longitudinal and lateral stability was evaluated by classical analysis methods and a study of historical trends.⁵ The horizontal tail and the location of the center of gravity were sized to provide static longitudinal stability.¹ The effects of expected gust induced loads in the longitudinal direction, pitch, results in a rate of change of the pitching moment with the total airplane lift (dC_M/dC_L) of -0.310, rendering static stability to the configuration.

Historical trends were studied,⁵ and a total dihedral angle of 2.5° was determined to ensure sufficient roll stability, while not hindering the collection of solar power. A compound dihedral angle was chosen. The dihedral angle begins at the modular wing connections. The modular wing sections are positioned at an angle of 5° , insuring a total dihedral angle of 2.5° . The vertical tail and dihedral were sized to provide lateral stability. The vertical tail has a Vertical Tail Volume Coefficient of approximately 0.02, typical for a sailplane. The tail has an area of 900 cm^2 , and furnishes directional stability.

The necessary control surface sizes for the plane were determined using a combination of historical trends for similar aircraft⁵ and recommendations taken from model aircraft publications. Approximately half of the vertical stabilizer surface area was removed and replaced by a rudder. The rear quarter of the horizontal stabilizer's chord is occupied by an elevator spanning the entire length (1 m) of this component. These control surfaces are actuated by Futaba electronic servos housed within the horizontal stabilizer. Due to the solar cell placement, the chord of the ailerons was limited. To conform to the limited width, the ailerons span the entire length of the modular wing sections. The servos that control them are located directly in front of the ailerons, adjacent to the modular wing connections.

Performance and Mode of Operation

Solar propulsion is very appealing on the basis that it is harmless to the environment and cost efficient. The performance of a vehicle, however, is very confined to the weather, time of day, location, season, and efficiency of its solar power system. The available solar cells for this aircraft configuration were not the most efficient or light weight, yet did allow for excess power for take-off and climb. A computer code was developed to predict the performance of the aircraft in level flight.

The aircraft is designed to climb in a circular flight path to an altitude of 50 m in approximately 5 minutes, as shown in Figure 19. This mission requires 5.5 complete revolutions about a 200 m field. The climb rate is a function of the angle of incidence between the sun and the solar cell array; the aircraft climbs at a rate of 0.06 m/s away from the sun and 0.02 m/s towards the sun.

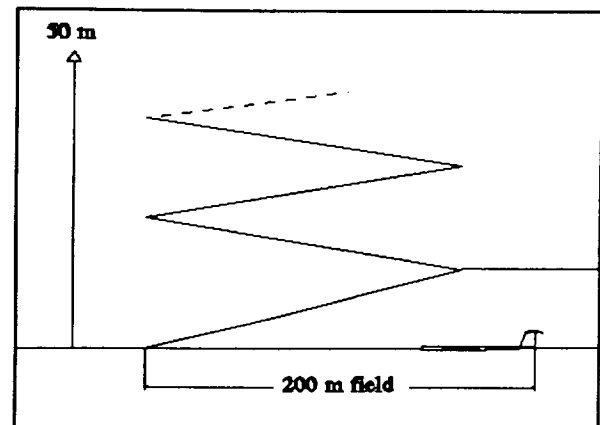


Fig. 19 Proposed Climb Scheme

At the design altitude, 18.8 W is required from the propulsion system to maintain flight at 7.1 m/s. A sustained figure eight flight pattern will be achieved with an angle of attack of 4° , banking angle between 3° and 4° , and a turning radius varying from 67 m to 89 m.

Results and Recommendations

Flight Testing

Surya underwent four flight tests between February and April of 1992. These tests proved not only to be valuable tools in the final design modifications but also as evidence of the sturdiness of the carbon composite structure. Due to the fragility of the solar cells, the first three test flights were completed before the cells were mounted. However, weights were used in place of the solar cells to estimate the behavior of the plane. The first flight test was without propulsion to verify that the location of the center of gravity was the same as that calculated theoretically. In this test, a slight wing twist was detected by the pilot, as well as a shift of the center of gravity from the desired location.

An overcorrected wing twist as well as another shift in the center of gravity persisted in the first powered flight test. The wing twist, now in the opposing direction, was again detected by the pilot. After adjustments were made to correct this by repositioning the modular wing sections, the plane proved to be responsive to controls and relatively easy to maneuver. The second powered flight test utilized the propeller's full power, and the need to optimize the propulsion system with a more efficient motor and propeller became evident. Again, the plane responded well to controls and flew for a short amount of time before landing quietly on simple yet effective landing skids.

In the fourth test flight, proxy cell weights were replaced by the actual solar cells. The wing twist was corrected as attested by the pilot. However, the new electronic components installed for the wiring of the cells shifted the center of gravity once again. This center of gravity shift and the presence of wind gusts caused the climb performance to be sluggish.

Recommendations

Many engineering difficulties were incurred during the design and construction of the solar plane, *Surya*. After the plane construction was completed, there appeared to be many components and processes which could be further optimized through more research, development, and testing. Of course many of these revelations were not obvious to the project team before the construction

began. The performance of *Surya* depends upon the following criteria: overall efficiency of the propulsion system, structural design, material selection, stability, aerodynamic analysis, and the overall weight of the plane.

The efficiency of the propulsion system is determined by its individual components including the solar cells, wiring, motor, propeller and the electronic configurations. It is obvious that the propulsion system is limited by the 12.5% efficient solar cells, but the system could be further optimized through improved matching of the motor and propeller. A more efficient motor along with a more powerful propeller would further optimize the propulsion system. To aid in the conservation of the weight budget, lighter wire could be used in the solar cell configuration.

Difficulties in maintaining the stability of the plane were experienced during flight testing. The center of gravity was not easily maintained at one tenth of the chord length. The majority of the stability problems could be eliminated by changing the propulsion configuration to include a pusher propeller. This configuration would enable the center of gravity to be kept ahead of the main wing and additional cells to be placed on the horizontal stabilizer. In addition to improved stability, the pusher propeller configuration would allow additional solar cells and power acquired from the cells.

Though *Surya* is structurally sound, the weight of the plane could greatly be reduced in most of the structural components. The handmade carbon composite fuselage and the wing and tail spars could be constructed more exactly to fully optimize the weight. The diameter of the fuselage could be reduced to conserve the weight of the plane. This dimension was originally dictated by a linkage used in the electronics. This linkage was later redesigned so that the fuselage diameter could be reduced. Many processes requiring the application of glue were done using epoxy, which tended to be heavier than standard superglue. Using the glue more sparingly would aid in the minimization of the weight of the plane.

The large size of the plane required that the wing sections of *Surya* be modular. The modular connections of the wing were constructed using a foam and carbon composite combination. These connections could be further optimized to conserve weight and possibly increase stability.

The control surfaces of the plane were increased in size to account for the increase in the size of the entire plane. After completion the plane seemed to be harder to control than had been anticipated. Enlarging the size of the control surfaces would aid in the overall performance of the plane.

The recommendations mentioned above indicate areas in which the design team felt limited. Most of these recommendations occurred at the completion of construction and were realized through experience. Further research and development in these areas are encouraged since the possibilities for various design configurations of this type of aircraft are numerous.

Environmental Impact

Society is faced with various self-induced environmental problems. Implementation of solar energy as a replacement of traditional energy resources provides an economical solution. The design and construction of this solar powered aircraft attempts to contribute to this cause and encourage future research into alternative energy resources.

Acknowledgments

The assistance and technical support of the NASA contacts, Mobil Solar, Aerospace Composites, faculty, staff, students, and many other interested aircraft modelling enthusiasts were numerous and very greatly appreciated. Special thanks to Art Glassman, our NASA/USRA mentor and the advising professors, Prof. William W. Durgin, Prof. Andreas N. Alexandrou, Prof. Ralph F. Cohn, Prof. David J. Olinger, Prof. Edward Clarke, and Kurt Heinzmann for their faithful guidance. The educating assistance on aircraft design vital to the required mission provided by Adam Szymkiewicz and Arthur Lavallee has been invaluable. Also thanks to the many helpful staff from WPI especially Todd Billings, Bob Taylor, and Roger Steele for sharing their expertise and equipment.

References

1. Shevell, R.S. Fundamentals of Flight, Prentice Hall, Englewood Cliffs NJ, 1989.
2. Selig et. al. Soartech 8: Airfoils at Low Speeds. H.A.
3. Kuethe, A. and Chow, C. Foundations of Aerodynamics, 4th Ed. John-Wiley and Sons: New York, 1986.
4. Hu, C. and White. R.M. Solar Cells From Basic to Advanced Systems. McGraw Hill: New York, 1983.
5. Raymer, D. Aircraft Design: A Conceptual Approach. AIAA, Inc.: Washington, DC, 1989.

